



Cite this: *React. Chem. Eng.*, 2020, 5, 1005

Received 25th March 2020,  
Accepted 21st April 2020

DOI: 10.1039/d0re00116c

rsc.li/reaction-engineering

## Beyond electrolysis: old challenges and new concepts of electricity-driven chemical reactors

Andrzej I. Stankiewicz <sup>\*ab</sup> and Hakan Nigar <sup>a</sup>

With renewable electricity becoming the most widespread, flexible, and accessible form of energy on Earth, electrification of chemical processes presents one of the most promising transition paths to low-carbon-footprint, environmentally-neutral manufacturing of fuels and chemicals. The current paper provides a critical perspective on the entire spectrum of chemical and catalytic reactors, in which electricity plays different roles targeting either the reaction mechanism or the thermal energy supply. Related challenges and necessary developments to address those challenges are discussed.

### Introduction

Decarbonization of the energy-intensive manufacturing industries presents one of the most urgent technological challenges of coming decennia. Among those industries, the chemical sector (including refineries) is by far the most significant energy consumer – according to the U.S. Energy Information Administration, in 2018, the bulk chemical and refining sectors were responsible for 46% of the entire energy consumption by the American industry.<sup>1</sup> The transition scenarios to the low-carbon energy in the chemical process industries are commonly based on the so-called power-to-X concept, which basically assumes using low-carbon or renewable electricity to produce fuels and/or chemicals.<sup>2–7</sup> However, in the vast majority of rich research literature related to those scenarios, the use of electricity is limited to the initial steps of electro(cata)lytic conversion of water, CO<sub>2</sub> and/or nitrogen, respectively to hydrogen, carbon monoxide, syngas, formic acid, methanol or ammonia.<sup>8–20</sup> The subsequent reaction steps are usually assumed to be carried out in the conventional, thermochemical way. While the electrocatalytic production of fuels from water, CO<sub>2</sub> or nitrogen is undoubtedly of fundamental importance for decarbonizing (or rather defossilizing) the chemical sector, it is equally important to address possible applications of electricity in the reactions further down the chain – the reactions that eventually lead to thousands of chemical products on the market today. With those reactions in mind, in the current paper we critically review the entire spectrum of relevant electricity-based chemical and catalytic reactors,

focusing on the related challenges and the new concepts to address them.

### Electricity roles in chemical and catalytic reactors

Generally speaking, electricity can be applied in a chemical reactor, either directly or indirectly. The latter means that the reactor utilizes another energy form, to which electricity is first converted, *e.g.*, microwave, light, *etc.* In either of the above, electricity can fulfil two distinct roles in a chemical reactor. On the one hand, it can target the reaction mechanism, usually switching it from the thermal to the non-thermal one, based on the electron/charge transfer. On the other hand, electricity can be used as a means for fast (and in some cases selective) energy supply to the thermally-driven reactions (Fig. 1).

Reactors belonging to the first category include:

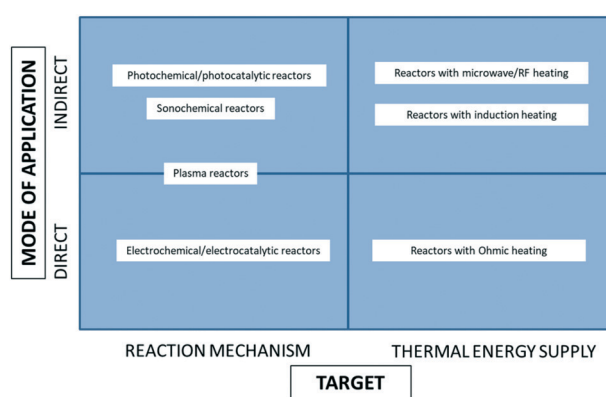


Fig. 1 Classification of the electricity-based reactors with respect to the mode of electricity application and its role in the reactor.

<sup>a</sup> Process and Energy Department, Delft University of Technology, Leeghwaterstraat 39, 2628 CB Delft, The Netherlands. E-mail: a.i.stankiewicz@tudelft.nl

<sup>b</sup> Faculty of Chemical and Process Engineering, Warsaw University of Technology, Waryńskiego 1, 00-645 Warsaw, Poland



- Electrochemical and electrocatalytic reactors, in which electric current (DC) is supplied directly to the electrodes causing charge transfer across the interface between the electrode and the processed liquid.

- Photochemical and photocatalytic reactors, in which electrical energy is converted to a mono- or polychromatic light, and the emitted photons produce either direct excitation of the reacting molecules or creation of the electron-hole pairs in the catalyst.

- Plasma reactors, in which electricity is used (directly or indirectly) to create highly reactive plasmas with a large number of chemically active species, such as electrons, ions, atoms, and radicals.

- Sonochemical reactors, in which electricity converted to ultrasound creates microcavitation and generates free radicals in the reacting liquid.

Thermal energy transfer in electricity-based reactors can be realized *via*:

- Microwave/RF heating, in which the rapidly alternating electric field of the microwave generates heat by moving dipolar molecules or ions in liquids, or by getting absorbed in the so-called “dielectric lossy” solid non-magnetic materials.

- Ohmic or Joule heating, in which the electric current passing through a resistive conductor produces heat.

- Induction heating, in which the rapidly alternating magnetic field either generates eddy currents in conducting materials resulting in the Joule heating of those materials, or generates heat in ferro-/ferrimagnetic materials by the magnetic hysteresis losses.

## Applications, challenges and new concepts of electricity-driven reactors

### Systems targeting reaction mechanism

**Electrochemical reactors.** With its more than one hundred years history of industrial applications, electrochemical reactors present the oldest category of reactors utilizing electricity as an energy source. Next to the flagship processes, such as aluminium or chloralkali production of chlorine, numerous electrochemical synthesis routes have already been

commercialized. Sequeira and Santos<sup>21</sup> reported not less than 31 commercial-scale organic electrosynthesis processes (of which the most well-known is adiponitrile synthesis), and another 19 processes carried out on the pilot scale.

Despite their long history and commercial successes, the design and scale-up of electrochemical reactors remain complex and challenging tasks, in which various elements address diverse general and application-specific design issues. Those essential elements of electrochemical reactor design are summarized in Table 1.

A great variety of electrochemical reactor concepts have been developed and implemented in industrial practice.<sup>22</sup> The more traditional include parallel-plate reactors, rotating-electrode reactors, “Swiss-roll-cell” reactors, as well as reactors with packed-bed or fluidized-bed electrodes.<sup>23</sup> More recently, BASF<sup>37</sup> presented a reactor for electrosynthesis of aromatic aldehydes, based on the “capillary gap” cell (Fig. 2a). The cell is constructed of a stack of bipolar round graphite electrodes with a central hole, separated by spacers. The electrolyte flows *via* the central channel created by the stacking and then outwards between the electrodes. Such a reactor design results in a high ratio of electrode surface area to reactor volume.

Somewhat similar in terms of the basic idea is the electrochemical pump cell based on rotating disc-type electrodes, that dates back to mid-1970s.<sup>38</sup> It has recently been further developed as the spinning disc membrane electrochemical reactors<sup>39</sup> (Fig. 2b). Here, the electrolytes are fed through the central channel and flow in the gap between the rotating electrode and the stator.

The most recent trend is the development of microfluidic flow devices for electrochemical synthesis.<sup>40–42</sup> Those devices overcome many traditional limitations associated with electrochemistry and can operate in serial or parallel mode (numbering-up). However, tiny volumes (below 1 mL) restrict their possible use for commercial-scale manufacturing.

**Photochemical and photocatalytic reactors.** Similarly to electrochemistry, photochemical processes have a long industrial history. Chlorinations of saturated hydrocarbons were the first photoreactions to be carried out on the industrial scale already before WWII.<sup>43</sup> Photo-oximation of cyclohexane, which was commercialized by Toyo Rayon (now Toray) in 1963, presents a well-known example of a bulk

**Table 1** Essential elements of electrochemical reactor design and issues/challenges they address

Design element	Issue/challenge addressed	Ref.
Reactor type/geometry	High electrode area per unit volume; high current density; low voltage; heat management; hydrodynamics	22–24
Electrode geometry and material	Uniform potential/current distribution; low voltage; electrode durability	25 and 26
Electrocatalyst	High reaction rate/selectivity; low overpotential	27–29
Electrode surface structure	Improved mass transfer	30–32
Diaphragm/membrane	High selectivity; improved product separation; reduced mixing of electrolytes and (gaseous) reaction products	22, 23 and 33–35
Electrolyte	Reduced energy losses Improved stability; high ionic conductivity; improved mass transfer	36



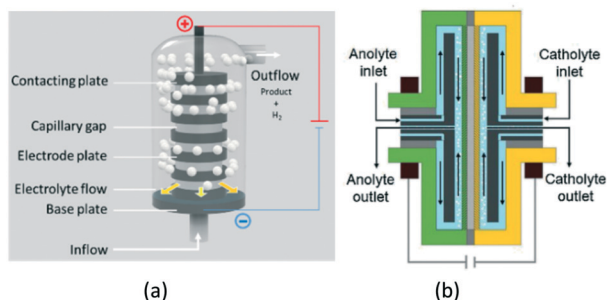


Fig. 2 Capillary gap cell (a) and rotor-stator spinning disc membrane electrochemical reactor (b). Fig. 2b reprinted from Granados Mendoza, *et al.*,<sup>39</sup> with permission from Elsevier.

(>170 kton per year) photochemical process.<sup>44</sup> Since then, many other photochemical reactions have been carried out industrially, ranging from the >500 kton per year halogenations down to a few ton per year production of fine chemicals or vitamin precursors.

Generally speaking, the use of light to activate chemical bonds may render two critical advantages compared to the traditional thermochemical processes:

- Process selectivity to the required products can drastically increase, due to the different chemistry, or low/ambient process temperature.
- The energy consumption in the process can radically decrease, due to the low-temperature processing.

However, in order to maximize the above advantages, important challenges related to quantum yield, light attenuation (Beer-Lambert law), and overall energy efficiency need to be resolved *via* the light source and reactor design.

A variety of light sources can be used in photochemistry,<sup>45</sup> with mercury lamps being still the most common solution in large-scale applications. The main features of the most relevant light sources used or studied in photochemical reactors are presented in Table 2.

The choice of the photoreactor type depends on different factors, including the phases present, the required production capacity, the reaction chemistry, and the physical properties of the reactants/solvents. The primary challenge in the reactor design is the efficiency of the photon transfer from the light source to target molecules or photocatalysts. In liquid-phase processes, immersion reactors are the most popular. A classic example here is the pool reactor for photo-oxidation of cyclohexane (see earlier), in which a multitude of immersed mercury lamps are used. The mercury lamps

generate large quantities of heat and are polychromatic. Therefore, they require filters and intensive cooling systems.

Much more efficient, in particular on the small-to-medium production scales, are continuous-flow photoreactors.<sup>46–49</sup> These reactors are commonly constructed of transparent plates with specially shaped micro- or millichannels and LED-matrices as the light sources. A typical representative of this category is the G3 Photo Reactor developed at Corning (Fig. 3). The reactor, made of glass, PFA, and perfluoroelastomer, has the maximum processing capacity of 2 l min<sup>-1</sup>. It uses monochromatic LED irradiation and provides efficient light penetration with both sides of fluidic modules illuminated. Efficient liquid cooling extends the LEDs lifetime. Corning claims the reactor to offer 1000 times better heat transfer, 100 times better mass transfer, 1000 times lower volume, and 50 times better residence time distribution than the batch reactor. Next to the G3 model, there are several other flow-chemistry photoreactors on the market, *e.g.*, PhotoCube™ (ThalesNano, Hungary) or PhotoSyn™ (Uniqsis, UK). Those reactors, however, have lower processing capacities and therefore are more suited for laboratory-scale applications.

Recently, a continuous-flow stirred-tank photoreactor with a fiber-coupled, high-powered diode laser as the light source has been investigated.<sup>50</sup> The reactor utilizes an adjustable beam expander to ensure uniform illumination of the liquid surface (Fig. 4). Running a C–N coupling reaction, the lab-scale device with only 100 ml volume has been able to operate at a throughput of 1.2 kg per day, which proves its potential for application in small-scale pharmaceutical manufacturing.

Additional challenges and design concepts are encountered in the photocatalytic processes running on solid photocatalysts. Here, not only the optimum positioning of the light source with respect to the catalyst surface but also the catalyst deposition on illuminated reactor elements, the specific illuminated surface area as well as general scalability of the device, play an essential role. A good overview of various photocatalytic reactor concepts that include flat plate, slurry, spinning disc, honeycomb monolithic, optical fiber, annular, packed-bed, fluidized-bed, and microreactors, can be found in Van Gerven *et al.*<sup>51</sup> and Khodadadian *et al.*<sup>52</sup>

A common hurdle in photocatalytic reactors is their limited energetic efficiency. This is due on the one hand to the light absorption and dissipation between the source and the catalytic site, and on the other hand to the “mismatch”

Table 2 Light sources for photochemical reactors

Light source	Wave lengths (approx.)	Radiant efficiency (approx.)	Lifetime till 70% intensity [h] (approx.)	Remarks
Mercury lamp	200–600 nm	0.32	2000–10 000	Polychromatic
Xenon lamp	200–2500 nm	0.80	2000	Polychromatic
Excimer lamp	108–350 nm; (most often 172 nm)	0.25–0.40	2000	Quasi monochromatic
Fluorescent black light	310–450 nm	0.25	20 000	Polychromatic
LED	210–900 nm	0.01–0.62	20 000	Quasi monochromatic
Laser	193–10 600	0.25	Up to 70 000 (time to failure)	True monochromatic





Fig. 3 Corning® Advanced-Flow™ G3 photo reactor (left) and G3 fluidic module (right). © 2018 and 2017 Corning Incorporated. All rights reserved. Reprinted with permission.

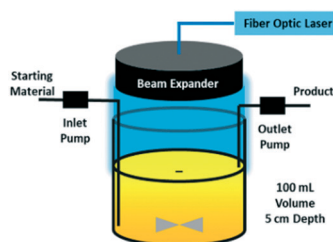


Fig. 4 Continuous stirred-tank photo reactor with fiber-coupled laser diode as the light source. Reprinted from Harper *et al.*,<sup>50</sup> with permission from ACS.

between the large bandgap of the photocatalyst (usually  $\text{TiO}_2$ ) and the visible light source, resulting in effective utilization of only a small UV-part of the emitted light. The ultimate solution to the light absorption/dissipation problem would be to generate the light directly in the catalyst or the solvent containing the reactants (“nano-illumination”). So far, that topic has attracted only limited attention. Gole *et al.*<sup>53</sup> proposed the introduction of nitrogen-doped titania nanostructures into the pores of porous silicon (PS) in order to develop a device generating visible light by electroluminescence of PS, thus activating the photocatalyst particles. This device could then be incorporated in a micro- or millireactor, as shown in Fig. 5. Another example of nanoscale illumination is the use of phosphorescent solids, which are irradiated prior to their injection in the reactant stream.<sup>54</sup> Much more abundant is the literature concerning the improvement (reduction) of the bandgap of the photocatalysts, where significant developments in the field of plasmonic catalysts are seen.<sup>55–57</sup>

Last but not least, the use of light and photocatalysts in photoelectrochemical cells needs to be mentioned. Those

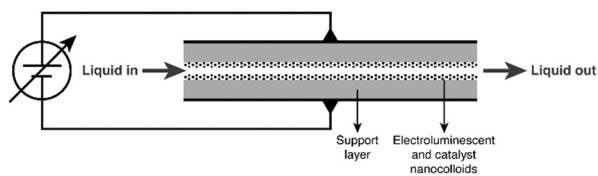


Fig. 5 Nanoscale illumination reactor. Source: Van Gerven *et al.*,<sup>51</sup> reprinted with permission from Elsevier.

cells are composed of a transparent anode coated with a nanostructured photocatalyst and a conventional cathode. Illumination of the anode generates electrons in the photocatalyst, which are then conducted *via* an external circuit to the cathode and carry out reduction reactions there. In contrast, the generated holes in the photoanode are used for carrying out oxidation reactions. Among potential applications of photoelectrochemical reactors, the production of hydrogen dominates the field.<sup>58–61</sup>

**Plasma reactors.** In 1969, Ibberson and Thring published a review paper on plasma engineering and processing.<sup>62</sup> The main conclusion and the subtitle of the paper reads: “Potential for chemical synthesis is high but still unrealized”. Today, fifty years later, the same conclusion holds. Since the 1940s thermal plasma-based H<sub>2</sub> process for hydrocarbon cracking to acetylene,<sup>63</sup> large-scale applications of plasmas in chemical manufacturing are quite scarce. Often quoted examples are environment-related and include dielectric barrier discharge (DBD)-based ozone generators for environmental applications<sup>64,65</sup> or pulsed corona-based incineration.<sup>66</sup> On the other hand, plasmas (in particular non-thermal ones) found numerous applications in materials processing (*e.g.* synthesis of inorganic materials, spraying, etching, CVD, polymerization or treatment of polymer surfaces) and in medicine (*e.g.* sterilization of surfaces, tissue engineering, wound healing or treatment of skin diseases). An excellent review of both realized and potential plasma applications can be found in Fridman’s monograph.<sup>67</sup>

The three basic challenges on the way to more industrial-scale applications of electricity-driven reactors, *i.e.* (i) energy efficiency, (ii) reaction selectivity/yield control, and (iii) reactor scale-up, are particularly pronounced in case of plasma reactors. Among all types of plasma, the microwave-induced plasma has the highest energy efficiency when operated under reduced pressure (~100–200 Torr) but that efficiency dramatically drops when moving to higher, industrially relevant pressures.<sup>68</sup> Delikonstantis and co-workers carried out a thorough analysis of alternative process options for the microwave plasma-based ethylene production from methane.<sup>69</sup> They found out that the break-even electricity prices for the process were in the range 23–35 USD per MW h, which is *circa* 2–4 lower than the current rates. Those figures were obtained for a nanosecond pulsed discharge reactor operating under an elevated pressure of 5 bar, which in other paper from the same group exhibited a *circa* order-of-magnitude better energy efficiency than the conventional microwave-plasma reactors.<sup>70</sup>

Reaction selectivity/yield control in plasma reactors is a problematic issue, mainly because of the vast numbers of vibrationally excited species and elementary reaction steps generated by the plasma. For example, full kinetic models of even such a “simple” microwave-plasma process as  $\text{CO}_2$  dissociation include 10 000+ reactions and 100+ species. Such highly complex models are practically useless when it comes to the design and scale-up of a reactor and model reduction methodologies need to be developed. One of such



methodologies resulted in the reduction of the CO<sub>2</sub> dissociation model to 44 reactions and 13 species.<sup>71</sup> In an attempt to improve product yield and selectivity, hybrid designs combining plasma with heterogeneous catalysis have been proposed. Dominant are fixed-bed systems, as the one for dry reforming of methane<sup>72</sup> shown in Fig. 6. It must be noted, however, that the interactions between plasma and a heterogeneous catalyst are very complex (Fig. 7) and therefore present as such a significant challenge, both in terms of their detailed understanding and the mathematical modelling.

Also, the microreactor technology offers opportunities for the improved control of plasma chemistries. Here, both non-catalytic and catalytic micro- and millichannel plasma reactors have been investigated.<sup>74–78</sup> Their expected advantages include low-power operation, improved heat transfer management, and in the case of catalytic reactors – very high surface areas offered and adequate addressing the short lifetimes of the vibrationally excited species.

The approach to plasma reactor scale-up depends primarily on two factors: the type of plasma concerned and the intended production scale. Most large-scale thermal plasma gasification processes base on a single reactor vessel equipped with multiple plasma torches. In the case of microwave plasma, the reaction chambers can be fitted with several microwave generators and stacked on each other,<sup>79</sup> as shown in Fig. 8a. In DBD plasma reactors, on the other hand, the numbering-up strategy prevails, that results in multitubular assemblies, as in the case of ozone generators<sup>80</sup> (Fig. 8b).

**Sonochemical reactors.** Using ultrasound for intensification of chemical reactions has been investigated for many years. First reports on chemical and biological rate enhancement by the ultrasound were published in the late 1920s. Since the early 1980s, the field of sonochemistry has become a very popular area of (mostly) chemical research. Ultrasound-generated microcavitation has been shown to

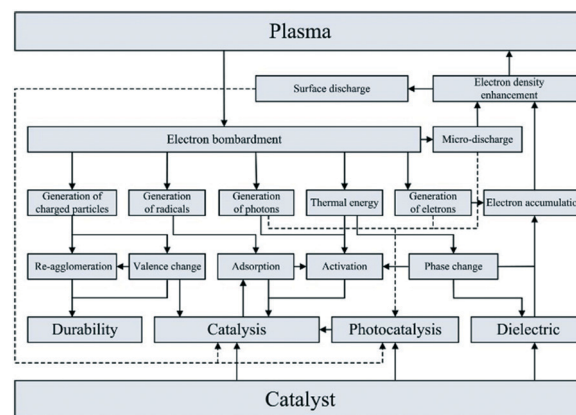


Fig. 7 Interactions between plasma and heterogeneous catalyst. Source: Chung and Chang;<sup>73</sup> reprinted with permission from Elsevier.

dramatically speed up many liquid-phase reactions, as has been reported in the excellent paper by Thompson and Doraiswamy.<sup>81</sup> A unique feature of the ultrasound, as compared to other electricity-based technologies, is its ability of not only affecting the reaction mechanisms/rates by the enormous microscale energy release and generation of free radicals, but also the enhancement of the mass transfer rates, both in the gas–liquid and liquid–solid systems.<sup>82–85</sup> The reduction of the boundary layer thickness due to the micro-scale turbulence and the reduction of the viscosity in

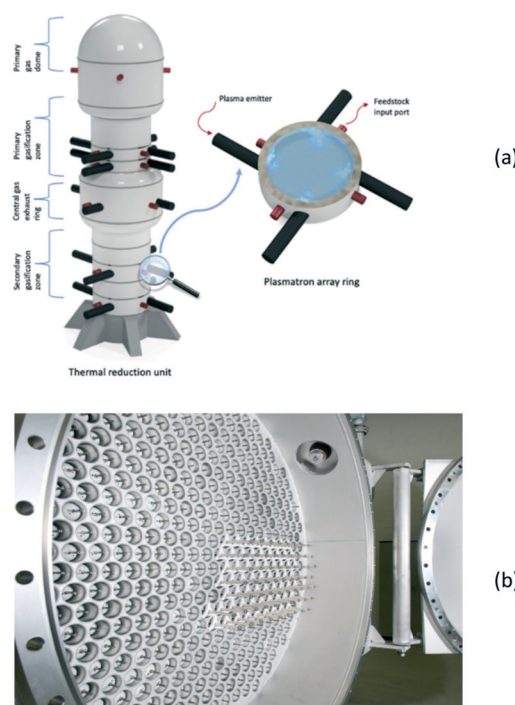


Fig. 8 Scale-up of a MW-plasma reactor by stacking reactor chambers with multiple microwave generators (a), and numbering-up of DBD reactor tubes (b). Fig. 8b: © 2020 SUEZ. All rights reserved. Reprinted with permission.

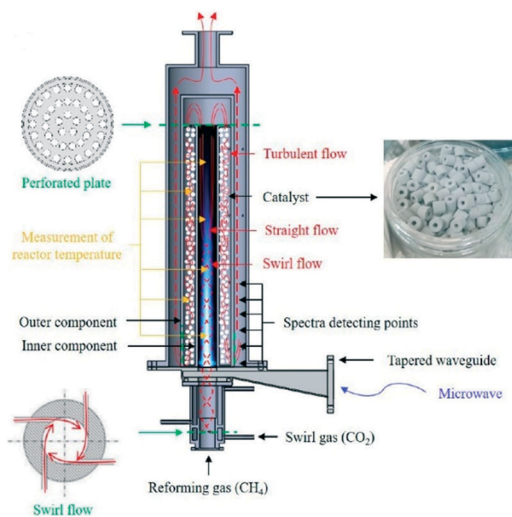


Fig. 6 Fixed-bed catalytic plasma reactor for dry reforming of methane. Reprinted from Chun *et al.*,<sup>72</sup> with permission from MDPI.



the boundary layer are the usually postulated mechanisms behind the observed phenomenon.

Despite the above-said features and despite *circa* four decades of research, industrial-scale applications of ultrasound in the chemical synthesis are yet to be seen. The challenges and technology development issues are as old as the technology itself and include:

- Stochastic character of the cavitation events, which makes modelling and scale-up extremely difficult.
- Lack of understanding of the relation between a cavitation collapse and chemical reactivity.
- Limited control of cavitation intensity.
- Small penetration depth of acoustic waves.
- Equipment erosion due to cavitation.
- Capacity and stability of ultrasound transducers.
- Low overall energetic efficiency (lower than in hydrodynamic cavitation reactors).

In order to address at least a part of the above challenges, various ultrasonic reactor designs have been proposed. In flow-cell reactors, the characteristics and the distribution of ultrasonic transducers, the vessel geometry, as well as the material/structure of the reactor wall play the role. Various types of magnetostrictive and piezoelectric transducers and their characteristics are discussed in the comprehensive review by Yao, *et al.*<sup>85</sup> Among reactor geometries, hexagonal flow cells with triple-frequency transducers<sup>86</sup> and rectangular flow cells with single-frequency transducers<sup>87</sup> have been investigated on bench- and pilot-scales. Fernandez Rivas and co-authors<sup>88,89</sup> proposed a soft-wall reactor called cavitation intensifying bag (CIB), in which the inner surface of the wall was modified with patterned pits of microscopic dimensions (Fig. 9). The patterned generation of microcavities from the pits resulted in significantly increased overall cavitation activity and energy efficiency.

Another path to follow, in particular for small-scale applications, is to combine the ultrasound with

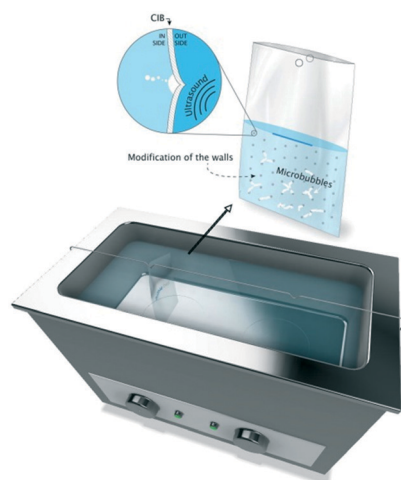


Fig. 9 Cavitation intensifying bag reactor with patterned micropits in the walls. Source: Van Zwieten *et al.*<sup>89</sup> Reprinted with permission from Elsevier.

microchannel reactor systems that offer short diffusion paths and high specific interfacial area resulting in increased mass transfer rates in multiphase reactions.<sup>90</sup> Three different approaches are reported in the literature, of which the simplest is a microreactor capillary immersed in an ultrasonic bath<sup>91</sup> (Fig. 10). The other two consist in having the reactor capillary in a direct or interval contact with an aluminium plate located on an ultrasonic transducer<sup>92</sup> (Fig. 11). The interval contact can further include a temperature control medium flowing in the gap between the reaction tube and the aluminium plate.<sup>93</sup>

### Systems targeting thermal energy supply

**Microwave reactors.** The research on the application of microwave (and radiofrequency) heating to chemical reactions started in the 1980s with the pioneering works by Gedye and co-workers.<sup>94</sup> Initially, the literature concerned the intensification of chemical reactions in liquid-phase systems (mostly organic synthesis and polymerizations), and there are several good reviews on this subject.<sup>95–100</sup> Later on, the research on the use of microwaves in gas-phase heterogeneous catalysis has started.<sup>101</sup> Those two categories of reactions (liquid-phase and gas–solid) need to be mentioned and analysed separately, as the interaction mechanisms, effects and the related challenges are different in both cases.

In liquids, the microwave energy transfer is realized *via* rotational or translational movements of, respectively, dipoles or ions in the fast-oscillating electric field component of the microwave, which causes internal friction and results in what we call the “volumetric heating”. In solid catalysts, on the other hand, the situation is more complex. Next to the dipolar dielectric loss (interaction of local dipoles, *e.g.*, –OH, –NH<sub>3</sub> groups, within the crystal lattice), conduction losses (interaction of ions, *e.g.* Na<sup>+</sup>, within the lattice) resulting from the charge carrier processes occur. Also, magnetic losses due to the interaction of the magnetic moment of the material with the magnetic field component of the microwave radiation may result in (additional) heating. Due to the above-described complexity, the response of a solid material to the microwave heating is often difficult to predict. In this

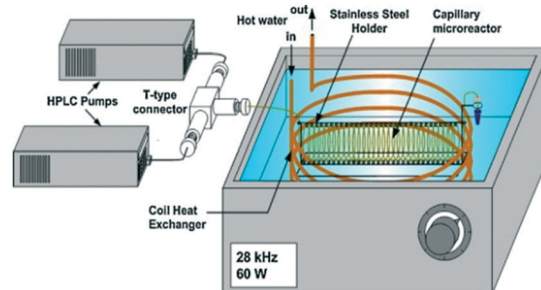
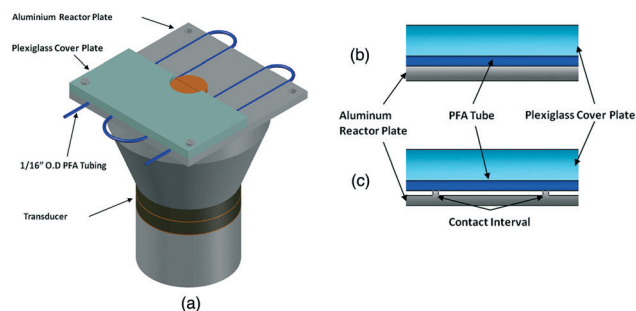


Fig. 10 Ultrasound-assisted microreactor with the reaction tube immersed in the ultrasonic bath. Source: Aljbour, *et al.*<sup>91</sup> Reprinted with permission from Elsevier.





**Fig. 11** Ultrasound-assisted microreactor (a) with direct (b) or interval (c) contact between the reactor tube and the transducer. Source: John, *et al.*<sup>92</sup> Reprinted with permission from Elsevier.

regard, Nigar *et al.*<sup>102</sup> developed a 3D mathematical model for a microwave heating system to predict the electric field distribution, axial and radial fixed-bed temperature profiles and temperature evolution with time for one of the widely used solid heterogeneous catalyst, *i.e.*, NaY zeolite. The fixed-bed temperature evolution under non-steady state conditions showed the same trend as the one observed experimentally with only an average deviation of 10.3%. They highlighted that knowing the dielectric characterization of materials is crucial for predicting the heating profiles. Irrespectively of that, however, the microwave heating of solid catalysts offers interesting opportunities from the reaction engineering viewpoint: (i) one can selectively heat-up the metal nanoclusters within an otherwise microwave-neutral catalyst support,<sup>103</sup> and (ii) one can operate at bulk gas temperature much lower than the catalyst temperature, thereby limiting the occurrence of the unwanted, homogeneous side-reactions.<sup>104</sup>

Consequently, the main challenges in applying microwave reactors on the industrial scale are different in (gas)-liquid and gas-solid systems. In liquid systems, the primary challenge consists in bringing and releasing the microwave radiation inside the reactor. Irradiating the reactor content from outside through the reactor wall, *e.g.* by placing the vessel in a large microwave cavity, would suffer from the limited penetration depth of the microwave and would require a reactor constructed of a microwave-transparent



**Fig. 12** LABOTRON™ microwave reactor with internal transmission line for liquid-phase reactions. © 2020 Sairem S.A. All rights reserved. Reprinted with permission.

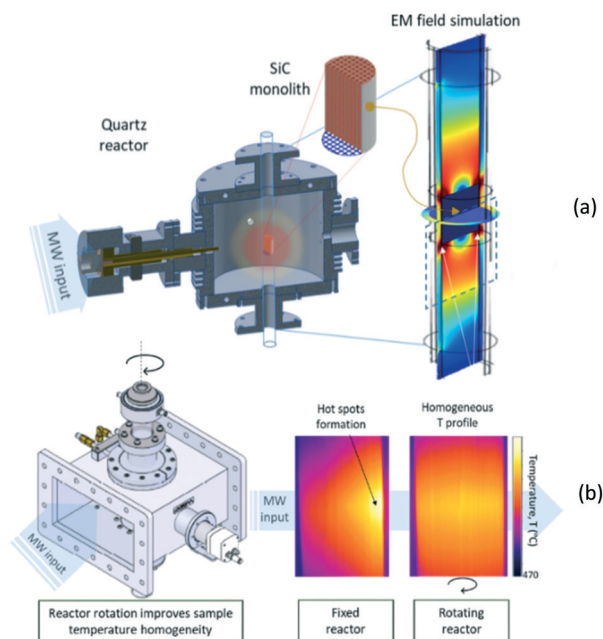


**Fig. 13** Monomodal microwave reactor; (a) – general scheme; (b) – heating uniformity improvement achieved by monolith rotation (courtesy: University of Zaragoza).

material, *e.g.*, quartz, PTFE. An alternative reactor concept addressing the above challenge is presented in Fig. 12. It is the so-called internal transmission line system commercialized by company Sairem under the name LABOTRON™. In this system, the microwave is fed through a U-shaped waveguide and transmitted into the reactor *via* the internal transmission line that is placed in the middle of the vessel in direct contact with the reaction mixture. This allows overcoming the penetration depth limitation. The reactor itself can be made of steel, can operate under elevated pressure, and can be equipped with a cooling jacket.

In heterogeneously catalysed gas-phase reactions, on the other hand, the main challenge consists in achieving uniform heating of the catalyst, as conventional microwave irradiation

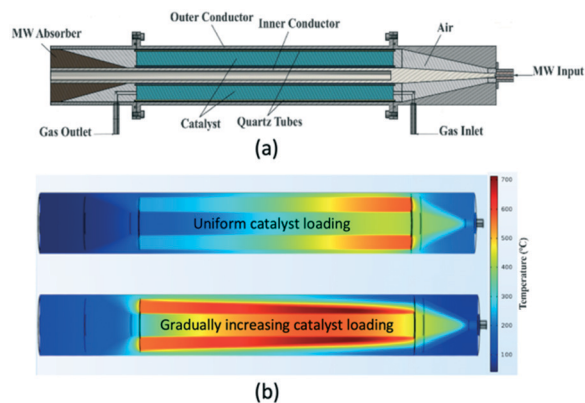
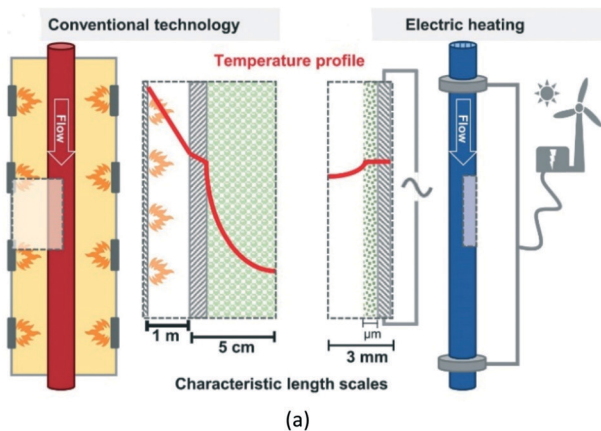
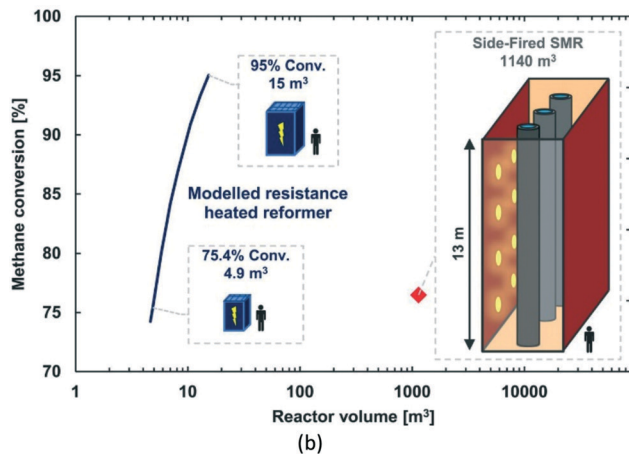


**Fig. 14** Traveling microwave reactor; (a) – scheme; (b) – heating profiles at different catalyst loading patterns: uniform and gradually increasing.





(a)



(b)

Fig. 15 Electric resistance-heated methane steam reformer; (a) – operational principle compared to conventional technology; (b) – possible miniaturization degree of the reactor as a function of the target methane conversion. Source: Wismann, *et al.*<sup>111</sup> Reprinted with permission from American Association for the Advancement of Science.



Fig. 16 Induction-preheated reactor for catalytic cracking. Source: Archibald, *et al.*<sup>112</sup> Reprinted with permission from American Chemical Society.

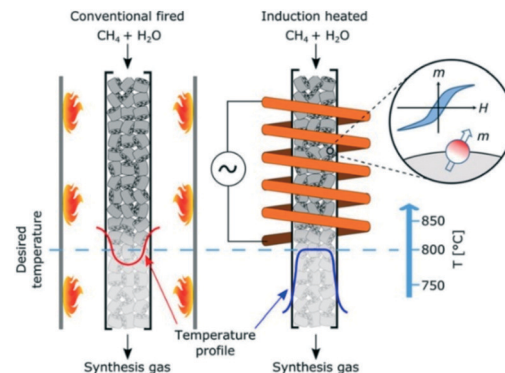


Fig. 17 Induction-heated catalytic reactor for methane steam reforming.<sup>120</sup> Source: Mortensen, *et al.*<sup>120</sup> Reprinted with permission from American Chemical Society.

of a bed of catalyst particles has been shown to result in very large temperature gradients, in the range of  $100 \text{ K cm}^{-1}$ .<sup>101,105</sup> Recently, two different reactor concepts have been developed that address the above challenge. The operational principle of the monomodal microwave reactor (MMR),<sup>106</sup> developed at the University of Zaragoza in collaboration with the University of Valencia, is creation of a standing microwave in a specially designed cavity (Fig. 13a) and heating of a monolithic catalyst, in which the endothermic reaction takes place. In order to increase the uniformity of the heating, the same group at Zaragoza together with Danish Technological Institute implemented the rotation of the monolithic catalyst inside the cavity (Fig. 13b).

A different reactor concept, the so-called traveling microwave reactor has been developed and investigated at Delft University of Technology.<sup>107</sup> In this reactor the microwave is allowed to “travel” co-currently to the reacting gas through a bed of catalyst. The bed is positioned in the annular space between two conductors (Fig. 14a), and the non-dissipated fraction of the microwave is absorbed by a specially designed absorber at the reactor outlet. Because of the full cylindrical symmetry, the TMR ensures uniform temperature distribution in the tangential direction at each cross-section of the catalyst bed. By manipulating the catalyst distribution/voidage, a uniform longitudinal temperature profile in the bed can be obtained (Fig. 14b).

**Resistance-heated reactors.** Ohmic heating, also known as Joule heating, has quite a long research history in food processing. In the area of reaction engineering, however, the literature on this type of energy transfer mechanism is scarce, with only a few papers published in the recent years.<sup>108–111</sup> Among other things, Pinto *et al.*<sup>109</sup> have shown that Ohmic heating not only could shorten the reaction time with respect to the traditional oil bath but was also able to deliver significantly higher yields than the microwave heating for various organic synthesis reactions in water. Another interesting concept has been presented is the recent *Science* paper by Wismann and co-authors,<sup>111</sup> who proposed a new, electric resistance-heated reactor for the steam reforming of



Table 3 Applicability of various electricity-driven reactor types

Reactor type	Commercially applied?/feasible production scales	Scale-up difficulty	Phases present (G-gas; L-liquid; S-solid)			
			G	(G)/L	G/S	(G)/L/S
Electrochemical	YES/small to very large	Intermediate		O		O
Photochemical	YES/small to large	Intermediate		O	O	O
Plasma	YES/small to large	Difficult	O		O	
Sonochemical	NO/small to medium	Difficult		O		O
Microwave-heated	YES/small to medium	Difficult		O	O	O
Resistance-heated	NO/small to large	Intermediate	O		O	
Induction-heated	NO/small to large	Intermediate	O	O	O	O

methane. The most important advantage of the new reactor type lies in significantly smaller radial temperature gradients in a thin catalyst layer on the tube wall when compared to a conventional fire-heated tube with a fixed bed of catalyst particles inside (Fig. 15a). The modelling study has shown that it could potentially lead to considerable miniaturization of the reformer, as shown in Fig. 15b.

**Induction-heated reactors.** Compared to the resistance-heated reactors, the induction-heated reactors have attracted more attention in the literature. This concerns both heating mechanisms involved in the induction heating: the more intensive eddy currents-based mechanism in conductive materials, and the less intensive hysteresis-based mechanism in magnetic materials.

Reactor concepts utilizing induction heating have quite a long history. The first publication related to this topic dates from 1952 and comes from Shell.<sup>112</sup> The researchers investigated the possibility of using the induction heating for a very fast preheating of petroleum fractions entering a catalytic cracking unit. Such a fast preheating to very high temperatures (700 °C or more) should help to reduce thermal cracking and coke formation on the catalyst. Accordingly, an induction-heated cracking unit was designed and investigated. In the unit shown in Fig. 16, the catalyst bed is preceded by a preheater consisting of an induction coil and a bundle of gold wires. In the preheater, petroleum fractions were heated up from 400 to 700 °C in about 10 milliseconds. As a result, carbon formation in the novel reactor was less than 1/10th of that in a conventional system.

More recently, induction-heated stirred-tank<sup>113</sup> and fluidized-bed<sup>114</sup> reactor concepts, both using the eddy currents mechanism, were proposed.

The majority of reactors utilizing the hysteresis-based induction heating are packed-bed flow systems filled with magnetic catalyst particles. The group of Kirschning<sup>115–117</sup> investigated inductive heating in relation to organic synthesis in microreactors. The heating in the reactor channels was realized *via* superparamagnetic core-shell nanoparticles, *e.g.*, silica-coated manganese ferrite particles. This led to significantly shorter reaction times and higher yields than in the corresponding batch reactors. Also, an important advantage mentioned by the authors was the simplicity of the induction-heated microreactor in comparison with its microwave-heated counterpart. Rebrov and co-workers<sup>118</sup>

designed and investigated a hysteresis-heated micro-trickle-bed reactor for two-step conversion of citronella to menthol, while the group of Chaudret carried out continuous CO<sub>2</sub> hydrogenation in magnetically-induced flow reactor filled with composite iron carbide nanoparticles.<sup>119</sup> Finally, Mortensen and co-workers<sup>120</sup> demonstrated a catalytic flow reactor system for methane steam reforming, using induction-heated supported magnetic nickel-cobalt nanoparticles (Fig. 17). The Co-component of the catalyst with high Curie temperature provided enough heat to carry out high-temperature endothermic reaction catalysed by the Ni-component.

## Conclusions

At dawn of the renewable electricity age, chemical reactor engineering has developed plurality of electricity-driven reactor concepts utilizing various energy transfer mechanisms. Those concepts cover not only the electrochemical conversion of water, CO<sub>2</sub>, and nitrogen to hydrogen, syngas or ammonia, but are applicable to a broad range of chemical and catalytic reactions at various production scales – see Table 3.

The technology maturity (or technology readiness level, TRL) of the electricity-driven reactors varies widely from the proof-of-concept stage (*e.g.* sonochemical reactors) up to commercially operating large-scale units (*e.g.* photoreactors). The most important challenges in further development include spatial and temporal control of the electricity-generated fields, design and fabrication of energy-responsive catalysts, and overall energetic efficiency. To address those challenges, a more intensive multidisciplinary research involving catalysis, physics, materials science, electrical and chemical engineering is necessary. Better fundamental understanding of the underlying phenomena and interrelations will result in the development of novel energy-responsive catalysts and reactor systems with enhanced field control. Also, standard chemical reaction engineering courses in university curricula will need to be modernized, to include more elements of electricity-based reactor modelling and design.

With renewable electricity becoming the most widely available, versatile energy form on Earth, the electricity-driven reactors discussed in the present paper will play a



crucial role in the transition to green, environmentally-neutral manufacturing of fuels and chemicals. Circa 3.5 billion years ago, electricity might have triggered the appearance of life on Earth.<sup>121,122</sup> Electricity in chemical reactors may nowadays help preserve life on Earth for ages to come.

## Conflicts of interest

There are no conflicts to declare.

## References

- 1 U.S. Energy Information Administration, Annual Energy Outlook 2019I, January 2019 (<https://www.eia.gov/energyexplained/use-of-energy/industry.php>).
- 2 S. Lechtenböhmer, L. J. Nilsson, M. Åhman and C. Schneider, *Energy*, 2016, **115**, 1623–1631.
- 3 D. Parra, X. Zhang, C. Bauer and M. K. Patel, *Appl. Energy*, 2017, **193**, 440–454.
- 4 S. R. Foit, I. C. Vinke, L. G. J. de Haart and R.-A. Eichel, *Angew. Chem., Int. Ed.*, 2017, **56**, 5402–5411.
- 5 C. Wulf, J. Linssen and P. Zapp, *Energy Procedia*, 2018, **115**, 367–378.
- 6 H. Blanco, W. Nijs, J. Ruf and A. Faaij, *Appl. Energy*, 2018, **232**, 617–639.
- 7 J. Guilera, J. R. Morante and T. Andreu, *Energy Convers. Manage.*, 2018, **162**, 218–224.
- 8 F. M. Sapountzi, J. M. Garcia, C. J. Weststrate, H. O. A. Friedriksson and J. W. Niemantsverdriet, *Prog. Energy Combust. Sci.*, 2017, **58**, 1–35.
- 9 M. Schalenbach, A. R. Zeradjanin, O. Kasian, S. Cherevko and K. J. J. Mayrhofer, *Int. J. Electrochem. Sci.*, 2018, **13**, 1173–1226.
- 10 N. Mahmood, Y. Yao, J.-W. Zhang, L. Pan, X. Zhang and J.-J. Zou, *Adv. Sci.*, 2018, **5**, 1700464.
- 11 H. R. Jhong, S. Ma and P. J. A. Kenis, *Curr. Opin. Chem. Eng.*, 2013, **2**, 191–199.
- 12 C.-T. Dinh, T. Burdyny, M. G. Kibria, A. Seifitokaldani, C. M. Gabardo, F. P. Garcia de Arquer, A. Kiani, J. P. Edwards, P. De Luna, O. S. Bushuyev, C. Zou, R. Quintero-Bermudez, Y. Pang, D. Sinton and E. H. Sargent, *Science*, 2018, **360**, 783–787.
- 13 M. Jouny, W. Luc and F. Jiao, *Ind. Eng. Chem. Res.*, 2018, **57**, 2165–2177.
- 14 O. Gutiérrez Sánchez, Y. Y. Birdja, M. Bulut, J. Vaes, T. Breugelmanns and D. Pant, *Curr. Opin. Green Sustain. Chem.*, 2019, **16**, 47–56.
- 15 F. Zhang, H. Zhang and Z. Liu, *Curr. Opin. Green Sustain. Chem.*, 2019, **16**, 77–84.
- 16 T. Burdyny and W. A. Smith, *Energy Environ. Sci.*, 2019, **12**, 1442–1453.
- 17 W. A. Smith, T. Burdyny, D. A. Vermaas and H. Geerlings, *Joule*, 2019, **3**, 1822–1834.
- 18 V. Kyriakou, I. Garagounis, E. Vasileiou, A. Vourros and M. Stoukides, *Catal. Today*, 2017, **286**, 2–13.
- 19 L. Wang, M. Xia, H. Wang, K. Huang, C. Quian, C. T. Maravelias and G. A. Ozin, *Joule*, 2018, **2**, 1055–1074.
- 20 R. Zhao, H. Xie, L. Chang, X. Zhang, X. Zhu, X. Tong, T. Wang, Y. Luo, P. Wei, Z. Wang and X. Sun, *EnergyChem*, 2019, **1**, 100011.
- 21 C. A. Sequeira and D. M. F. Santos, *J. Braz. Chem. Soc.*, 2009, **20**, 387–406.
- 22 K. Scott, *Dev. Chem. Eng. Miner. Process.*, 1993, **1**, 71–117.
- 23 R. J. Marshall and F. C. Walsh, *Surf. Technol.*, 1985, **24**, 45–77.
- 24 F. C. Walsh and D. Pletcher, in *Developments in Electrochemistry: Science Inspired by Martin Fleischmann*, ed. D. Pletcher, Z.-Q. Tian and D. E. Williams, J. Wiley & Sons, 2014, pp. 95–11.
- 25 F. Walsh and G. Reade, *Analyst*, 1994, **119**, 791–796.
- 26 A. H. Sulaymon and A. H. Abbar, in *Electrolysis*, ed. J. Kleperis and V. Linkov, In-Tech Opne, 2012, pp. 189–202.
- 27 D. Pletcher, *J. Appl. Electrochem.*, 1984, **14**, 403–415.
- 28 J. O. M. Bockris, *J. Serb. Chem. Soc.*, 2005, **70**, 475–487.
- 29 N. Munichandraiah, *J. Indian Inst. Sci.*, 2010, **90**, 261–270.
- 30 C. M. A. Brett and A. M. C. F. Oliveira Brett, in *Surface Engineering*, ed. R. Kossowsky and S. C. Singhal, Springer, Dordrecht, 1984, pp. 656–664.
- 31 N. Menzel, E. Ortel, R. Kraehnert and P. Strasser, *ChemPhysChem*, 2012, **13**, 1385–1394.
- 32 W. Zhu, R. Zhang, F. Qu, A. M. Asiri and X. Sun, *ChemCatChem*, 2017, **9**, 1721–1743.
- 33 S. Vasudevan, *Res. J. Chem. Sci.*, 2013, **3**, 1–3.
- 34 H. Jaroszek and P. Dydo, *Open Chem.*, 2015, **14**, 1–19.
- 35 M. Paidar, V. Fateev and K. Bouzek, *Electrochim. Acta*, 2016, **209**, 737–756.
- 36 D. E. Blanco and M. A. Modestino, *Trends in Chemistry*, 2019, **1**, 9–10.
- 37 N. Aust, in *Encyclopedia of Applied Electrochemistry*, ed. G. Kreysa, K. Ota and R. F. Savinell, Springer, New York, 2014, pp. 1392–1397.
- 38 M. Fleischmann, R. E. W. Jansson, G. A. Ashworth and P. J. Eyre, *British Pat.*, 1504690, 1974.
- 39 P. Granados Mendoza, S. MoshtariKhah, A. S. Langenhan, M. T. de Groot, J. T. F. Keurentjes, J. C. Schouten and J. van der Schaaf, *Chem. Eng. Res. Des.*, 2017, **128**, 120–129.
- 40 F. J. Del Campo, *Electrochem. Commun.*, 2014, **45**, 91–94.
- 41 M. A. Modestino, D. Fernandez Rivas, M. S. H. Hashemi, J. G. E. Gardeniers and D. Psaltis, *Energy Environ. Sci.*, 2016, **9**, 3381–3391.
- 42 G. Laudadio, W. De Smet, L. Struik, Y. Cao and T. Noël, *J. Flow Chem.*, 2018, **8**, 157–165.
- 43 W. Hirschkind, *Ind. Eng. Chem.*, 1949, **41**, 2749–2752.
- 44 Y. Ito and S. Matsuda, *Ann. N. Y. Acad. Sci.*, 1969, **147**, 618–624.
- 45 M. Sender and D. Ziegenbalg, *Chem. Ing. Tech.*, 2017, **89**, 1159–1173.
- 46 Y. Su, N. J. W. Straathof, V. Hessel and T. Noël, *Chem. – Eur. J.*, 2014, **20**, 10562–10589.
- 47 S. Elgue, T. Aillet, K. Loubiere, A. Conté, O. Dechy-Cabaret, L. Prat, C. R. Horn, O. Lobet and S. Vallon, *Chim. Oggi*, 2015, **33**(5), 58–61.



- 48 D. Cambié, C. Bottecchia, N. J. W. Straathof, V. Hessel and T. Noël, *Chem. Rev.*, 2016, **116**, 10276–10341.
- 49 K. Loubiere, M. Oelgemoeller and T. Aillet, *Chem. Eng. Process.*, 2016, **104**, 120–132.
- 50 K. C. Harper, E. G. Moschetta, S. V. Bordawekar and S. J. Wittenberger, *ACS Cent. Sci.*, 2019, **5**, 109–115.
- 51 T. Van Gerven, G. Mul, J. Moulijn and A. Stankiewicz, *Chem. Eng. Process.*, 2007, **46**, 781–789.
- 52 F. Khodadadian, M. Nasalevich, F. Kapteijn, A. I. Stankiewicz, R. Lakerveld and J. Gascon, in *Alternative Energy Sources for Green Chemistry*, ed. G. D. Stefanidis and A. I. Stankiewicz, The Royal Society of Chemistry, 2016, pp. 227–269.
- 53 J. L. Gole, A. Fedorov, P. Hesketh and C. Burda, *Phys. Status Solidi C*, 2004, **1**, S188–S197.
- 54 P. Ciambelli, D. Sannino, V. Palma, V. Vaiano and R. S. Mazzei, *Photochem. Photobiol. Sci.*, 2011, **10**, 414–418.
- 55 P. Wang, B. Huang, Y. Daia and M.-H. Whangbo, *Phys. Chem. Chem. Phys.*, 2012, **14**, 9813–9825.
- 56 X. Zhang, Y. L. Chen, R.-S. Liu and D. P. Tsai, *Rep. Prog. Phys.*, 2013, **76**, 046401.
- 57 K. H. Leong, A. A. Aziz, L. C. Sim, P. Saravanan, M. Jang and D. Bahnemann, *Beilstein J. Nanotechnol.*, 2018, **9**, 628–648.
- 58 M. Grätzel, *Nature*, 2001, **414**, 338–344.
- 59 P. Lianos, *Appl. Catal., B*, 2017, **210**, 235–254.
- 60 P. Dias and A. Mendes, in *Encyclopedia of Sustainability, Science and Technology*, ed. R. A. Meyers, Springer, 2018, pp. 1–52, DOI: 10.1007/978-1-4939-2493-6\_957-1.
- 61 M. Ahmed and I. Dincer, *Int. J. Hydrogen Energy*, 2019, **44**, 2474–2507.
- 62 V. J. Ibberson and M. W. Thring, *Ind. Eng. Chem.*, 1969, **61**(11), 48–61.
- 63 P. Pässler, W. Hefner, K. Buckl, H. Meinass, A. Meiswinkel, H.-J. Wernicke, G. Ebersberg, R. Müller, J. Bässler, H. Behringer and D. Mayer, in *Ullmann's Encyclopedia of Industrial Chemistry*, Wiley-VCH, 2008, vol. 1, pp. 277–326.
- 64 U. Kogelschatz, *Plasma Chem. Plasma Process.*, 2003, **23**, 1–46.
- 65 T. Kuroki, H. Fujishima, K. Otsuka, T. Ito, M. Okubo, T. Yamamoto and K. Yoshida, *Thin Solid Films*, 2008, **516**, 6704–6709.
- 66 H.-H. Kim, *Plasma Processes Polym.*, 2004, **1**, 91–110.
- 67 A. Fridman, *Plasma Chemistry*, Cambridge, 1st edn, 2008.
- 68 A. Bogaerts, T. Kozák, K. Van Laer and R. Snoeckx, *Faraday Discuss.*, 2015, **183**, 217–232.
- 69 E. Delikonstantis, M. Scapinello and G. D. Stefanidis, *Processes*, 2019, **7**, 68.
- 70 M. Scapinello, E. Delikonstantis and G. D. Stefanidis, *Fuel*, 2018, **222**, 705–710.
- 71 J. F. De la Fuente, S. H. Moreno, A. I. Stankiewicz and G. D. Stefanidis, *React. Chem. Eng.*, 2016, **1**, 540–554.
- 72 S. M. Chun, D. H. Shin, S. H. Ma, G. W. Yang and Y. C. Hong, *Catalysts*, 2019, **9**, 292.
- 73 W.-C. Chung and M.-B. Chang, *Renewable Sustainable Energy Rev.*, 2016, **62**, 13–31.
- 74 C. Trionfetti, A. Ağır, J. G. E. Gardeniers, L. Lefferts and K. Seshan, *J. Phys. Chem. C*, 2008, **112**, 4267–4274.
- 75 A. Ağır, L. Lefferts and J. G. E. Gardeniers, *IEEE Trans. Plasma Sci.*, 2009, **37**, 985–992.
- 76 A. Ağır, T. Nozaki, M. Nakase, S. Yuzawa, K. Okazaki and J. G. E. Gardeniers, *Chem. Eng. J.*, 2011, **167**, 560–566.
- 77 G. Schelcher, C. Guyon, S. Ognier, S. Cavadias, E. Martinez, V. Taniga, L. Malaquin, P. Tabelaing and M. Tatoulian, *Lab Chip*, 2014, **14**, 3037–3042.
- 78 J. Wengler, S. Ognier, M. Zhang, E. Levernier, C. Guyon, C. Ollivier, L. Fensterbank and M. Tatoulian, *React. Chem. Eng.*, 2018, **3**, 930–941.
- 79 J. F. De la Fuente, A. A. Kiss, M. T. Radoiu and G. D. Stefanidis, *J. Chem. Technol. Biotechnol.*, 2017, **92**, 2495–2505.
- 80 C. Wei, F. Zhang, Y. Hu, C. Feng and H. Wu, *Rev. Chem. Eng.*, 2017, **33**, 49–89.
- 81 L. H. Thompson and L. K. Doraiswamy, *Ind. Eng. Chem. Res.*, 1999, **38**, 1215–1249.
- 82 A. Kumar, P. R. Gogate, A. B. Pandit, H. Delmas and A. M. Wilhelm, *Ind. Eng. Chem. Res.*, 2004, **43**, 1812–1819.
- 83 U. Neis, *TU Hamburg-Harburg Reports on Sanitary Engineering*, 2002, vol. 35, pp. 79–90.
- 84 F. Laugier, C. Andriantsiferana, A. M. Wilhelm and H. Delmas, *Ultrason. Sonochem.*, 2008, **15**, 965–972.
- 85 Y. Yao, Y. Pan and S. Liu, *Ultrason. Sonochem.*, 2019, DOI: 10.1016/j.ultsonch.2019.104722, in press.
- 86 P. R. Gogate, S. Mujumdar and A. B. Pandit, *Adv. Environ. Res.*, 2003, **7**, 283–299.
- 87 A. S. Mhetre and P. R. Gogate, *Chem. Eng. J.*, 2014, **258**, 69–76.
- 88 D. Fernandez Rivas, B. Verhaagen, A. Galdamez Perez, E. Castro-Hernandez, R. van Zwieten and K. Schroën, *J. Phys.: Conf. Ser.*, 2015, **656**, 012112.
- 89 R. van Zwieten, B. Verhaagen, K. Schroën and D. Fernández Rivas, *Ultrason. Sonochem.*, 2017, **36**, 446–453.
- 90 S. Hübner, S. Kressirer, D. Kralisch, C. Bludszuweit-Philipp, K. Lukow, I. Jänich, A. Schilling, H. Hieronymus, C. Liebner and K. Jähnisch, *ChemSusChem*, 2012, **5**, 279–288.
- 91 S. Aljbour, T. Tagawa and H. Yamada, *J. Ind. Eng. Chem.*, 2009, **15**, 829–834.
- 92 J. J. John, S. Kuhn, L. Braeken and T. Van Gerven, *Chem. Eng. Process.*, 2017, **113**, 35–41.
- 93 J. J. John, S. Kuhn, L. Braeken and T. Van Gerven, *Chem. Eng. Res. Des.*, 2017, **125**, 146–155.
- 94 R. Gedye, F. Smith, K. Westaway, H. Ali, L. Baldisera, L. Laberge and J. Rousell, *Tetrahedron Lett.*, 1986, **27**, 279–282.
- 95 C. O. Kappe, *Angew. Chem., Int. Ed.*, 2004, **43**, 6250–6284.
- 96 M. Nüchter, B. Ondruschka, W. Bonrath and A. Gum, *Green Chem.*, 2004, **6**(3), 128–141.
- 97 C. O. Kappe and E. Van der Eycken, *Chem. Soc. Rev.*, 2010, **39**, 1280–1290.
- 98 D. Bogdal and A. Prociak, *Gendai Kagaku*, 2007, **25**, 42–44.
- 99 R. Hoogenboom and U. Schubert, *Macromol. Rapid Commun.*, 2007, **28**, 368–386.



- 100 C. Ebner, T. Bodner, F. Stelzer and F. Wiesbrock, *Macromol. Rapid Commun.*, 2011, **32**, 254–288.
- 101 T. Durka, T. Van Gerven and A. Stankiewicz, *Chem. Eng. Technol.*, 2009, **32**, 1301–1312.
- 102 H. Nigar, G. S. J. Sturm, B. Garcia-Baños, F. L. Peñaranda-Foix, J. M. Catalá-Civera, R. Mallada, A. Stankiewicz and J. Santamaría, *Appl. Therm. Eng.*, 2019, **155**, 226–238.
- 103 X. Zhang, D. O. Hayward and D. M. P. Mingos, *Ind. Eng. Chem. Res.*, 2001, **40**, 2810–2817.
- 104 A. Ramirez, J. L. Hueso, M. Abian, M. U. Alzueta, R. Mallada and J. Santamaria, *Sci. Adv.*, 2019, **5**, eaau9000.
- 105 I. de Dios García, A. Stankiewicz and H. Nigar, *Catal. Today*, 2020, accepted.
- 106 I. Julian, H. Ramirez, J. L. Hueso, R. Mallada and J. Santamaria, *Chem. Eng. J.*, 2019, **377**, 119764.
- 107 F. Eghbal Sarabi, M. Ghorbani, A. Stankiewicz and H. Nigar, *Chem. Eng. Res. Des.*, 2020, **153**, 677–683.
- 108 S. Roux, M. Courel, L. Picart-Palmade and J.-P. Pain, *J. Food Eng.*, 2010, **98**, 398–407.
- 109 J. Pinto, V. L. M. Silva, A. M. G. Silva, A. M. S. Silva, J. C. S. Costa, L. M. N. B. F. Santos, R. Enes, J. A. S. Cavaleiro, A. A. M. O. S. Vicente and J. A. C. Teixeira, *Green Chem.*, 2013, **15**, 970–975.
- 110 J. Li, X. Lu, F. Wu, W. Cheng, W. Zhang, S. Qin, Z. Wang and Z. You, *Ind. Eng. Chem. Res.*, 2017, **56**, 12520–12528.
- 111 S. T. Wisman, J. S. Engbæk, S. B. Vendelbo, F. B. Bendixen, W. L. Eriksen, K. Aasberg-Petersen, C. Frandsen, I. Chorkendorff and P. M. Mortensen, *Science*, 2019, **364**, 756–759.
- 112 R. C. Archibald, N. C. May and B. S. Greensfelder, *Ind. Eng. Chem.*, 1952, **44**, 1811–1817.
- 113 V. Fireteanu, B. Paya, J. Nuns, Y. Neau, T. Tudorache and A. Spahiu, *COMPEL - The international journal for computation and mathematics in electrical and electronic engineering*, 2005, **24**, 324–333.
- 114 M. Latifi and J. Chaouki, *AIChE J.*, 2015, **61**, 1507–1523.
- 115 S. Ceylan, C. Friese, C. Lammel, K. Mazac and A. Kirschning, *Angew. Chem., Int. Ed.*, 2008, **47**, 8950–8953.
- 116 S. Ceylan, L. Coutable, J. Wegner and A. Kirschning, *Chem. – Eur. J.*, 2011, **17**, 1884–1893.
- 117 A. Kirschning, L. Kupracz and J. Hartwig, *Chem. Lett.*, 2012, **41**, 562–570.
- 118 S. Chatterjee, V. Degirmenci and E. V. Rebrov, *Chem. Eng. J.*, 2015, **281**, 884–891.
- 119 A. Bordet, L.-M. Lacroix, P.-F. Fazzini, J. Carrey, K. Soulantica and B. Chaudret, *Angew. Chem., Int. Ed.*, 2016, **55**, 15894–15898.
- 120 P. M. Mortensen, J. S. Engbæk, S. B. Vendelbo, M. F. Hansen and M. Østberg, *Ind. Eng. Chem. Res.*, 2017, **56**, 14006–14013.
- 121 S. L. Miller, *Science*, 1953, **117**, 528–529.
- 122 S. L. Miller and H. C. Urey, *Science*, 1959, **130**, 245–251.

